ONCOIMMUNOLOGY
2022, VOL. 11, NO. 01, e2148374 (11 pages)
https://doi.org/10.1080/2162402X.2022.2148374

Taylor & Francis
Taylor & Francis Group

ORIGINAL RESEARCH

Comprehensive evaluation of the tumor immune microenvironment and its dynamic changes in patients with locally advanced rectal cancer treated with preoperative chemoradiotherapy: From the phase II ADORE study

Hyungwoo Cho[a*], Jeong Eun Kim[a*], Yong Sang Hong[a], Sun Young Kim[a], Jihun Kim[b], Yeon-Mi Ryu[c], Sang-Yeob Kim[c], and Tae Won Kim[a]

[a]Departments of Oncology, Asan Medical Center, University of Ulsan College of Medicine, Seoul, Korea; [b]Departments of Pathology, Asan Medical Center, University of Ulsan College of Medicine, Seoul, Korea; [c]Asan Institute for Life Sciences, Asan Medical Center, University of Ulsan College of Medicine, Seoul, Korea

ABSTRACT

A better understanding of the effects of preoperative chemoradiotherapy (CRT) on tumor immune microenvironment (TIME) is essential to improve the treatment outcomes of patients with locally advanced rectal cancer (LARC). In this context, we performed a multiplex immunofluorescence staining to evaluate the TIME in 158 patients with LARC who underwent preoperative CRT followed by surgery and adjuvant chemotherapy in the ADORE trial. We found that higher levels of T-cell subsets ($CD3^+$, $CD4^+$, and $CD8^+$) and dendritic cells in the tumor compartment of pretreatment biopsy samples were associated with good response to preoperative CRT. After CRT, there was a significant increase in the densities of $CD3^+$ T cells, $CD8^+$ T cells, and dendritic cells, while that of $CD4^+FoxP3^+$ regulatory T cells decreased, indicating that CRT changed the TIME into a more immune-active status. However, CRT also conferred an immunosuppressive effect by polarizing the tumor-associated macrophages from pro-inflammatory M1 macrophage to immune-suppressive M2 macrophages and decreasing the density of B cells. High delta values of $CD3^+$ T cells and PD-$L1^+$ lymphocytes after CRT were associated with good disease-free survival (DFS), while that of $CD4^+FoxP3^+$ regulatory T cells was associated with poor DFS. These findings provide a framework for future studies incorporating strategies to modulate the TIME in patients with LARC.

ARTICLE HISTORY
Received 1 June 2022
Revised 2 November 2022
Accepted 11 November 2022

KEYWORDS
Rectal cancer; tumor immune microenvironment; chemoradiotherapy

Introduction

Preoperative chemoradiotherapy (CRT) followed by total mesorectal excision with or without adjuvant chemotherapy has been the standard treatment strategy for patients with locally advanced rectal cancer (LARC).[1–3] Recently, the total neoadjuvant therapy approach that incorporates chemotherapy with CRT prior to surgery has been proposed as a new treatment strategy.[4] Although these multimodality treatment strategies have led to significant improvements in the survival outcomes of patients with LARC, approximately 20% to 40% of the patients still experience disease progression.[4–7] Therefore, more efforts are needed to identify patients with poor prognosis and optimize the treatment strategies.

The clinical importance of the tumor immune microenvironment (TIME) is increasing as the immune cells in the tumor microenvironment have been shown to be significantly associated with disease progression and sensitivity of tumors to therapeutic agents in various types of cancers including rectal cancer.[8–10] Multiple studies have demonstrated the prognostic value of immune cell subpopulations such as T cells, B cells, and tumor-associated macrophages in rectal cancer.[9–12] High density of $CD8^+$ T cells and $CD20^+$ B cells in TIME were associated with good survival outcomes, while the high density of M2 macrophages was associated with poor survival outcomes. Furthermore, a recent study reported that a decrease in $CD8^+$ T cell/$FoxP3^+$ tumor-infiltrating lymphocyte ratio after preoperative radiotherapy was associated with a better survival outcome, demonstrating that the dynamic changes in the TIME may affect treatment outcomes.[9] However, most of the previous studies on TIME in rectal cancer have evaluated only a limited number of immune cell subpopulation types, which may limit a clear assessment of the role of specific immune cell populations. Furthermore, with the increasing role of immune checkpoint inhibitors and other immunotherapy strategies in various types of cancer, understanding how radiation therapy or chemoradiotherapy affects the TIME is essential to advance treatment strategies in patients with LARC. Nevertheless, there are only few studies that evaluated the effect of preoperative CRT on the TIME in patients with LARC, and these studies have evaluated only a limited population of immune cells.[9,10]

The ADORE trial (ClinicalTrials.gov identifier: NCT00807911) was a randomized, open-label, multicenter, phase II trial that compared the efficacy of adjuvant fluorouracil and leucovorin (FL) with that of oxaliplatin plus

CONTACT Tae Won Kim twkimmd@amc.seoul.kr Department of Oncology, Asan Medical Center, University of Ulsan College of Medicine, 88 Olympic-ro 43-gil, Songpa-gu, Seoul, Korea

*These authors contributed equally to this work and should be considered co-first authors

Supplemental data for this article can be accessed online at https://doi.org/10.1080/2162402X.2022.2148374

fluorouracil and leucovorin (FOLFOX) in patients with postoperative ypStage II (ypT3-4N0) or ypStage III (ypTanyN1-2) rectal cancer after fluoropyrimidine-based preoperative CRT and total mesorectal excision.[5,6] The ADORE trial showed that patients treated with adjuvant FOLFOX had better DFS compared with patients treated with adjuvant FL, which served as the basis for adjuvant FOLFOX in becoming one of the standard adjuvant regimens in LARC patients with ypStage II or III disease after preoperative CRT and total mesorectal excision.

By analyzing the prospective cohort of the ADORE trial, this study aimed to comprehensively evaluate the 1) correlation between the TIME in pretreatment biopsy and response to preoperative CRT, 2) dynamic changes in the TIME after preoperative CRT, and 3) association between the TIME in post-preoperative CRT surgical specimen and survival outcomes, in LARC patients treated with preoperative CRT followed by total mesorectal excision and adjuvant chemotherapy.

Methods

Patients and histologic specimens

This is a prospective cohort study which included a total of 158 patients with postoperative ypStage II (ypT3-4N0) or III (ypTanyN1-2) rectal cancer after fluoropyrimidine-based preoperative CRT and total mesolectal excision who were treated at Asan Medical Center (Seoul, South Korea) and enrolled in the phase II ADORE trial between November 2008 and June 2012. Formalin-fixed paraffin-embedded (FFPE) tissue samples were obtained from both pretreatment biopsies and surgical resection specimens after CRT. Pretreatment biopsy specimens were available in 110 patients, surgical resection specimen after CRT was available in 144 patients, and paired pretreatment biopsy and surgical resection specimens were available in 101 patients (Figure 1a). All patients provided written informed consent for tissue collection. This study was approved by the institutional review board of Asan Medical Center.

Multiplex immunofluorescence staining

We performed multiplex immunofluorescence staining to comprehensively analyze the TIME of the pretreatment biopsy samples as well as the surgically resected samples after CRT. Rectal cancer specimens (4-μm sections) were cut from the FFPE blocks and transferred onto positively charged slides, followed by multiplex immunofluorescence staining with a Leica Bond Rx™ Automated Stainer (Leica Biosystems, Newcastle, UK). Briefly, the slides were baked for 30 min and dewaxed with Leica Bond Dewax solution (#AR9222, Leica Biosystems), followed by antigen retrieval with Bond Epitope Retrieval 2 (#AR9640, Leica Biosystems) in a pH 9.0 solution for 30 min. After antigen retrieval, slides were incubated with primary antibodies followed by secondary horseradish peroxidase-conjugated polymer. Each horseradish peroxidase-conjugated polymer created a covalent binding of a different fluorophore using tyramide signal amplification. This covalently bond reaction was followed by additional antigen retrieval with Bond Epitope Retrieval 1 (Cat #AR9961, Leica Biosystems, Milton Keynes, UK) for 20 min to remove prior primary and secondary antibodies before the next step in the sequence. Each slide was subjected to six sequential rounds of staining. After sequential reactions, sections were counterstained with Spectral DAPI and mounting with HIGHDEF® IHC fluoromount (Enzo Life Sciences, Farmingdale, NY).

Two panels were designed for multiplex immunofluorescence staining (Opal™ 7-color Automation IHC Kit; Akoya Biosciences, Marlborough, MA, USA), of which panel 1 included DAPI, CK, CD4, CD8, FoxP3, CD20, and PD-L1, and panel 2 included DAPI, CK, CD3, CD68, CD206, CD11c, and MHC class II (Figure 1, b and c). Further details of the panel information are summarized in Supplementary Table 1. $CD3^+$ was used for indicating T cells, $CD8^+$ for cytotoxic T cells, $CD4^+FoxP3^+$ for regulatory T cells, $CD4^+FoxP3^-$ for helper T cells, $CD20^+$ for B cells, $CD68^+CD206^-$ for M1 macrophages, $CD68^+CD206^+$ for M2 macrophages, CK-MHC II^+ for antigen-presenting cells, MHC II^+CD11c^+ for dendritic cells, and $CK^+PD\text{-}L1^+$ for PD-L1-positive tumor cells. Total lymphocyte count was calculated as the summation of $CD4^+$, $CD8^+$, and $CD20^+$ cells; $PD\text{-}L1^+$ lymphocyte count was calculated as the summation of $PD\text{-}L1^+CD4^+$, $PD\text{-}L1^+CD8^+$, and $PD\text{-}L1^+CD20^+$ cells; $PD\text{-}L1^-$ lymphocyte count was calculated as the summation of $PD\text{-}L1^-CD4^+$, $PD\text{-}L1^-CD8^+$, and $PD\text{-}L1^-CD20^+$ cells (Supplementary Figure 1).

Multiplex stained slides were scanned using the Vectra Polaris Automated Quantitative Pathology Imaging System (Akoya Biosciences, Marlborough, MA, USA) at 20× magnification. The regions of interest (ROIs) were carefully chosen by a pathologist specializing in colorectal cancer (J.K.) based on H&E slides and CK expression, and the size of each ROI was 0.64 mm^2. For pre-treatment biopsies, we selected at least two ROIs with evidence of tumor-associated microenvironment, which was defined by the presence of desmoplastic stroma and the degree of tumor-associated inflammation.[13] For surgically resected specimens after CRT, we first determined the invasive margin, which was the area within ± 0.5 mm perpendicular width (±, toward/away from the tumor center) along the invasive front as previously described in tumor-containing tissue sections.[14] Then, we chose 8–10 ROIs showing evidence of active tumor-stromal interaction, which includes tumor-associated microenvironment and singly scattered or small clusters of tumor cells. To accomplish this, we examined up to 4 tumor-containing sections per each surgically resected specimen.

Representative images for training were selected in Phenochart (Akoya Biosciences, Marlborough, MA, USA), and an algorithm was created in the inForm 2.4 Image Analysis software (Akoya Biosciences, Marlborough, MA, USA). Multispectral images were unmixed using the spectral library in inForm software, and all tissues were segmented according to the presence of CK antibody expression (Figure 1d, left). Based on DAPI staining, each single cell was segmented (Figure 1d, middle), and phenotyping was performed according to the expression compartment and intensity of each marker (Figure 1d, right). Batch analysis was performed on selected ROIs of all tissue using the same algorithm designed on representative images by the inForm Software.

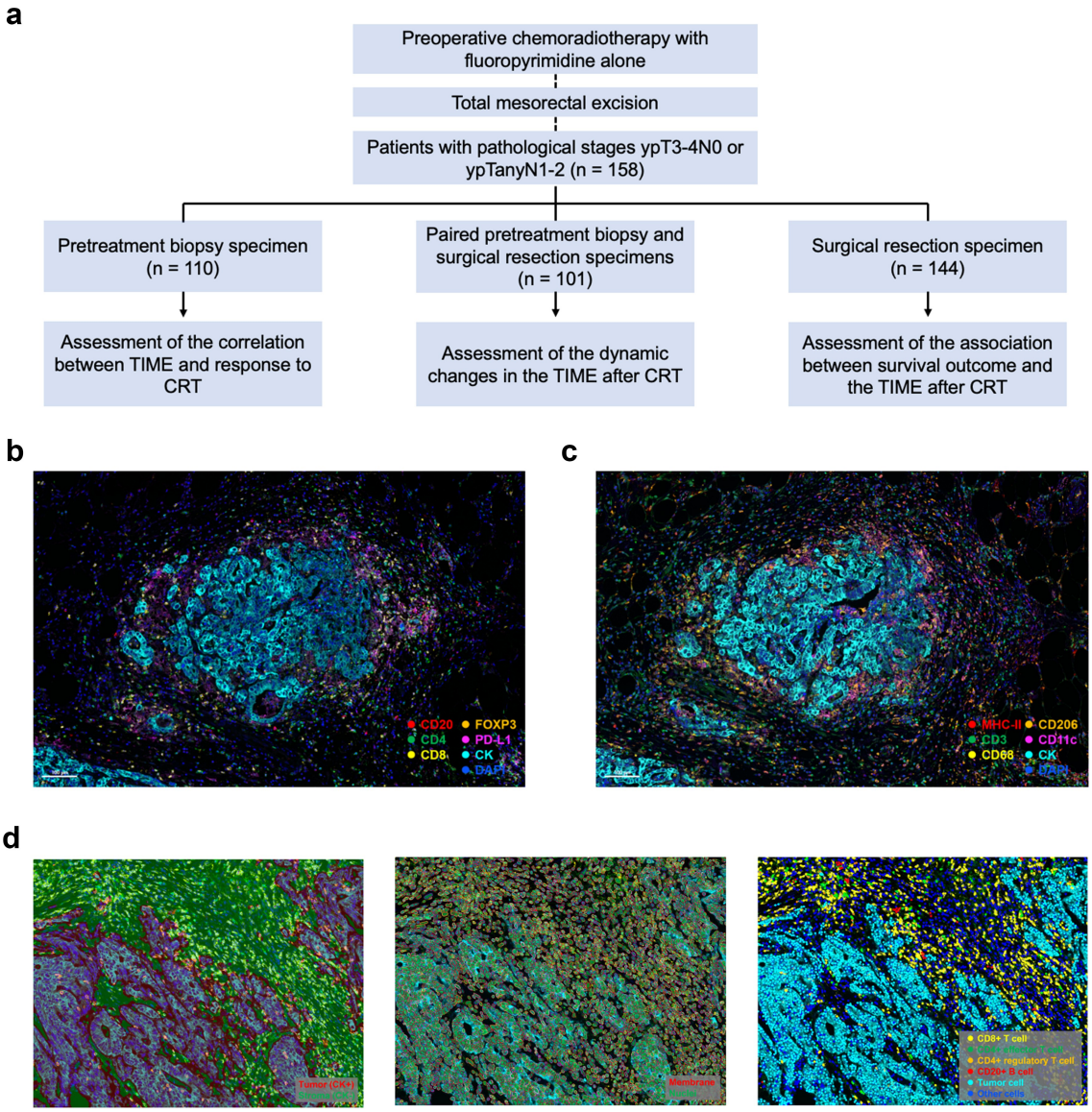

Figure 1. a, Cohort flow diagram. Representative examples of multiple immunofluorescence staining of rectal cancer. b, CK, CD4, CD8, FoxP3, CD20, PD-L1 (panel 1). c, CK, CD3, CD68, CD206, CD11c, MHC class II (panel 2). d, Analysis workflow of multiplex immunofluorescence staining: (d, left) tissue segmentation to differentiate tumor area (red) and the surrounding stroma (green); (d, middle) single cell segmentation (nuclei in green, and membrane in red); (d, right) cell phenotyping based on the detection of specific cell-surface or intracellular markers. Magnification, ×100. TIME, tumor immune microenvironment; CRT, chemoradiotherapy.

The exported data were consolidated and analyzed in R software using the phenoptr (Akoya Biosciences, Marlborough, MA, USA) and phenoptrReport packages (Akoya Biosciences, Marlborough, MA, USA). The counted cell numbers are expressed as the mean number of cells/mm^2 for each cell population.

In the biopsy specimens, we subdivided the regions into tumor area and the stromal area based on CK expression; in the surgical specimens, the entire tumor area including the regressed lesions was evaluated because it is difficult to accurately differentiate between the tumor and the stromal portion area after CRT. Similarly, when assessing the dynamic changes in TIME after preoperative CRT in patients with paired samples, the immune cell subpopulation in the tumor and the stromal areas were evaluated as a whole in both the biopsy specimens and post-treatment surgical specimens.

Cell-to-cell distance analysis

Topographic coordinates for each cell were obtained using the inForm software, and distance analyses were performed using Phenoptr and PhenoptrReports packages in R Studio (Akoya Biosciences). The consolidated data were used to calculate the nearest distance between tumor cells and specific immune cell subtypes within the desired radius. Then, the nearest distances were used together with the composite and component image data to visualize the spatial relationship. The nearest neighbor analysis was performed in pretreatment biopsy specimens (Supplementary Figure 2).

Tumor regression grade

Resected tumors after CRT were examined in their entirety and the degree of the regression of resected tumors was assessed by

estimating the percentage of residual viable tumor of the macroscopically identifiable tumor bed as identified in routine H&E staining. The extent of tumor regression was classified using the Dworak's tumor regression grading system:[15] TRG 0, no regression; TRG 1, dominant tumor mass with obvious fibrosis and/or vasculopathy; TRG 2, dominant fibrotic changes with few tumor cells or groups (easy to find); TRG 3, very few (difficult to find microscopically) tumor cells in fibrotic tissue with or without mucous substance; and TRG 4, no tumor cells and only a fibrotic mass (total regression or response).

Statistical analysis

Disease-free survival (DFS) was defined as the time from random assignment to documented recurrence or death, whichever occurred first. Overall survival (OS) was defined as the time from random assignment to the date of death from any cause. Survival rates and the corresponding standard errors were estimated using the Kaplan–Meier method, and survival curves were compared using the log-rank test. Differences between the TIME of pretreatment biopsy specimens according to TRG 0–2 vs. TRG 3–4 were compared using the Wilcoxon's rank-sum test (Mann–Whitney *U*-test), and the differences in TIME between the paired pretreatment biopsy specimen and surgical specimen after CRT were analyzed using Wilcoxon's signed-rank test. Univariate and multivariate analyses were performed using Cox proportional hazards regression modeling. Multivariate analysis included age, sex, and variables that exhibited a potential association with survival ($P < .2$) in the univariate analysis. The prognostic value of the dynamic changes in TIME was evaluated using delta parameters, which were the subtraction of immune cell subpopulation density after preoperative CRT minus its density at baseline (delta [Δ] = immune cell subpopulation density after preOP CRT – immune cell subpopulation density at baseline). The median value was used for determining the cutoff value for high (> median) and low (≤ median) immune cell density or delta parameters in the current study. All statistical calculations were conducted using R version 3.6.2. (R Foundation for Statistical Computing, Vienna, Austria, https://www.R-project.org/).

Results

Baseline characteristics

The baseline characteristics of the patients are presented in Table 1. The median age was 55.5 years (range, 25–81) and 116 (73.4%) patients were male. The median preoperative radiotherapy dose was 5000 cGy (range, 4500–5400), and all patients received fluoropyrimidine-based chemotherapy during preoperative radiotherapy followed by total mesorectal excision. Sixty-eight (43.0%) patients had ypStage II disease, and the remaining 90 (57.0%) had ypStage III disease. For adjuvant chemotherapy, 80 (50.6%) patients received fluorouracil plus leucovorin and 78 (49.4%) received FOLFOX. At a median follow-up duration of 87.2 months (95% CI, 82.8–91.8), the 5-year rates of DFS and OS were 60.0% (95% CI, 52.8–68.3) and 78.4% (95% CI, 72.2–85.1), respectively (Supplementary Figure 3).

TIME in pretreatment biopsy samples and response to preoperative CRT

The correlation between the TIME of pretreatment biopsy specimens and response to preoperative CRT was evaluated in 110 patients with available pretreatment biopsy samples (Supplementary Table 2, Figure 2). Of these patients, 22 (20.0%) had a good response to preoperative CRT (TRG 3–4) while 88 (80.0%) had a poor response (TRG 0–2). The immune cell subpopulations were evaluated separately in the tumor compartment (Figure 2a–g). The density of $CD3^+$ T cells, total $CD4^+$ T cells, $CD4^+FoxP3^+$ regulatory T cells, $CD4^+FoxP3^-$ helper T cells, $CD8^+$ T cells, dendritic cells, and PD-$L1^+$ lymphocytes in the tumor compartment was significantly higher in patients with a good response than in patients with a poor response ($P < .05$) (Figure 2a–g). In the stromal compartment, only the density of PD-$L1^+$ lymphocytes was significantly associated with the response to preoperative CRT, and higher density was associated with good response ($P = .009$) (Figure 2h). The density of M1 or M2 macrophages in both tumor and stromal compartments was not significantly associated with response to preoperative CRT (Supplementary Table 2). High density of tumor-infiltrating $CD4^+FoxP3^+$ regulatory T cells (> median) was associated with higher levels of $CD3^+$ T cells, $CD8^+$ T cells, $CD4^+FoxP3^-$ helper T cells, $CD20^+$ B cells, antigen-presenting cells, and dendritic cells compared with patients with a low density of tumor-infiltrating $CD4^+FoxP3^+$ regulatory T cells (Supplementary Table 3). We additionally explored the spatial distributions and interactions of tumor cells with respect to immune cells using the nearest neighbor analysis. Patients with a good response to preoperative CRT had a significantly shorter average distance between the tumor cells and $CD8^+$ T cells (Supplementary Table 4 & Supplementary Figure 4).

Dynamic changes in the TIME after preoperative CRT and their prognostic value for DFS

We then evaluated the dynamic changes in the TIME following preoperative CRT by analyzing paired pretreatment biopsy and surgical resection specimens from 101 patients (Figure 3, Supplementary Table 5). As for lymphocytes, the densities of $CD3^+$ T cells ($P = .03$) and $CD8^+$ T cells ($P < .001$) significantly increased after preoperative CRT, while those of $CD4^+FoxP3^+$ regulatory T cells and $CD20^+$ B cells significantly decreased (both $P < .001$) (Figure 3, a–d, Supplementary Table 4). There were no significant changes in the densities of total lymphocytes, PD-$L1^+$ lymphocytes, PD-$L1^-$ lymphocytes, and $CD4^+FoxP3^-$ helper T cells (Supplementary Table 5). As for tumor-associated macrophages, there was a significant decrease in the density of M1 macrophage, whereas the density of M2 macrophage significantly increased ($P < .05$ for all) (Figure 3, e and f, and Supplementary Table 5). For the remaining immune cell subpopulations, the density of dendritic cells increased significantly ($P < .05$), while there was no significant change in the density of antigen-presenting cells ($P = .74$)

Table 1. Baseline patient characteristics.

Characteristics	Patients with locally advanced rectal cancer treated with chemoradiotherapy (n = 158)
Age, median (range)	55.5 (25–81)
Sex, n (%)	
Male	116 (73.4%)
Female	42 (26.6%)
ECOG PS, n (%)	
0	1 (0.6%)
1	157 (99.4%)
Distance of the primary tumor from the anal verge (cm), n (%)	
≤ 4	49 (31.0%)
> 4 and ≤ 8	82 (51.9%)
> 8	27 (17.1%)
Histology, n (%)	
Well-differentiated	19 (12.0%)
Moderately differentiated	130 (82.3%)
Poorly differentiated, signet ring cell, mucinous	6 (3.8%)
Adenocarcinoma, NOS	3 (1.9%)
Preoperative radiotherapy, median dose in cGy (range)	5000 (4500–5400)
Concurrent chemotherapy during preoperative radiotherapy, n (%)	
Fluorouracil ± leucovorin	123 (77.8%)
Capecitabine	34 (21.5%)
UFT	1 (0.6%)
Type of surgery, n (%)	
Abdominoperineal resection	34 (21.5%)
Low anterior resection	121 (76.6%)
Hartmann's procedure	3 (1.9%)
Pathologic T stage, n (%)	
ypT0	3 (1.9%)
ypT1	4 (2.5%)
ypT2	13 (8.2%)
ypT3	134 (84.8%)
ypT4	4 (2.5%)
Pathologic N stage, n (%)	
ypN0	68 (43.0%)
yp1a	31 (19.6%)
yp1b	33 (20.9%)
yp2a	21 (13.3%)
yp2b	5 (3.2%)
ypStage, n (%)	
II	68 (43.0%)
III	90 (57.0%)
Lymphovascular invasion, n (%)	
Absent	132 (83.5%)
Present	24 (15.2%)
Unidentified	2 (1.3%)
Perineural invasion, n (%)	
Absent	119 (75.3%)
Present	37 (23.4%)
Unidentified	2 (1.3%)
Adjuvant chemotherapy, n (%)	
FL	80 (50.6%)
FOLFOX	78 (49.4%)

Abbreviations: ECOG PS, Eastern Cooperative Oncology Group Performance Status; NOS, not otherwise specified; UFT, uracil-tegafur; FL, fluorouracil plus leucovorin; FOLFOX, oxaliplatin plus fluorouracil and leucovorin.

(Supplementary Table 5). The dynamic change in TIME was similar between patients who achieved a good response to preoperative CRT (n = 16, Supplementary Figure 5, Supplementary Table 6) and those who achieved a poor response (n = 85, Supplementary Figure 6, Supplementary Table 7).

To evaluate the prognostic value of the dynamic changes in TIME after CRT, we used the delta parameters of the immune cell subpopulation. In univariate analysis, the delta values of $CD3^+$ T cells, $CD8^+$ T cells, $CD4^+FoxP3^+$ regulatory T cells, $CD20^+$ B cells, total lymphocytes, PD-$L1^+$ lymphocytes, and PD-$L1^-$ lymphocytes showed potential associations with DFS ($P < .2$) (Table 2). Among other clinical factors, age, ypN positivity, lymphovascular invasion, and perineural invasion showed potential association with DFS. In the multivariate analysis including variables with a potential association ($P < .2$) with DFS in the univariate analysis along with sex, high delta $CD3^+$ T cells (HR, 0.46; 95% CI, 0.22–0.98, $P = .043$) and high delta PD-$L1^+$ lymphocytes (HR, 0.39; 95% CI, 0.17–0.90, $P = .027$) were independently associated with good DFS, while high delta $CD4^+FoxP3^+$ regulatory T cell was associated with poor DFS (HR, 2.32; 95% CI, 1.09–4.92, $P = .028$). There were significant differences in 5-year DFS of patients with high vs. low delta $CD3^+$ T cells (75.5% vs. 52.3%, $P = .013$), delta

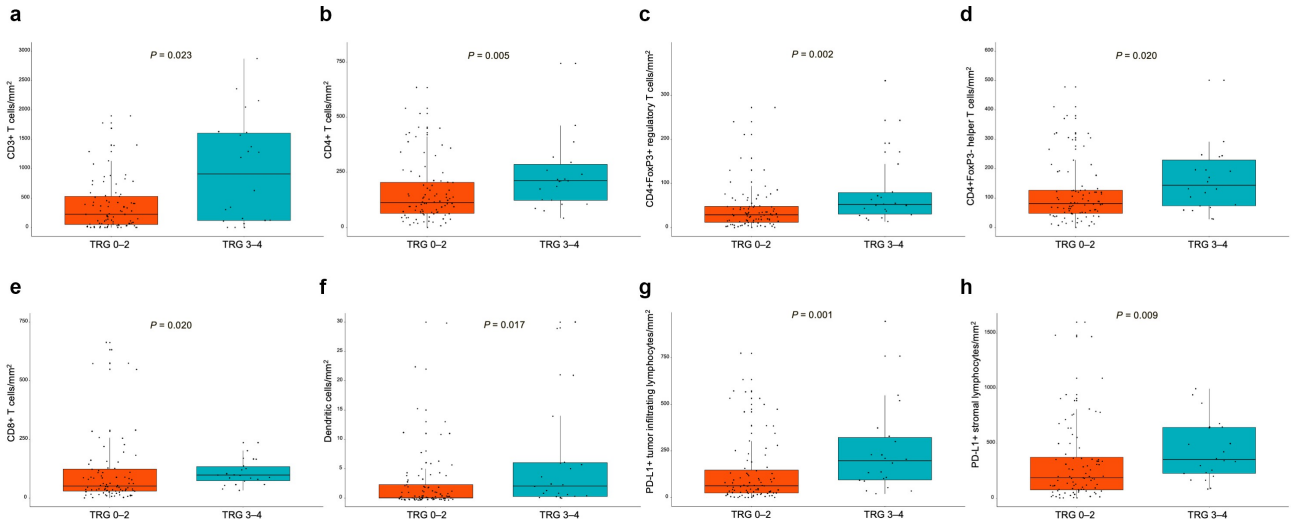

Figure 2. Correlations between the response to preoperative chemoradiotherapy and the immune cell populations in the tumor compartment (a-g) and stromal compartment (h) of pretreatment biopsy specimens. a, $CD3^+$ T cell. b, $CD4^+$ T cell. c, $CD4^+FoxP3^+$ regulatory T cell. d, $CD4^+FoxP3^-$ helper T cell. e, $CD8^+$ T cell. f, Dendritic cell. g, PD-L1 tumor-infiltrating lymphocyte. h, PD-L1+ stromal lymphocyte. Boxplots show the medians and the 25th and 75th percentiles; the whiskers extend from the hinge to the largest value no further than 1.5 × interquartile range from the hinge.

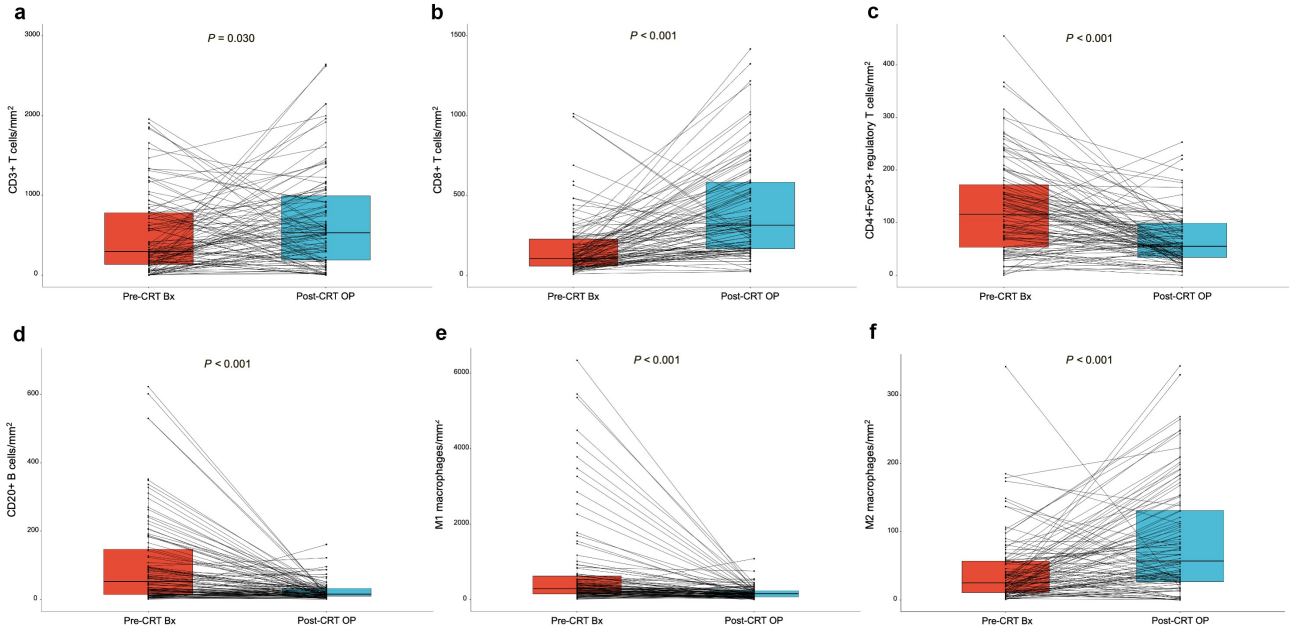

Figure 3. Dynamic changes in the tumor immune microenvironment after preoperative chemoradiotherapy. a, $CD3^+$ T cell. b, $CD8^+$ T cell. c, $CD4^+$ FoxP3+ regulatory T cell. d, $CD20^+$ B cell. e, M1 macrophage. f, M2 macrophage. Boxplots represent the medians and the 25th and 75th percentiles; the whiskers extend from the hinge to the largest value no further than 1.5 × interquartile range from the hinge.

CD4+ $FoxP3^+$ regulatory T cells (53.0% vs 74.5%, P = .033), and delta $PD\text{-}L1^+$ lymphocytes (77.2% vs. 51.4%, P = .005) (Figure 4)

Association between DFS and the TIME in surgical resection samples after CRT

We further evaluated the prognostic value of immune cell subpopulations in the TIME after preoperative CRT in 144 patients with available surgical resection specimens. In the multivariate analysis including age, sex, and variables with a potential association (P < .2) with DFS in the univariate analysis, high density of $PD\text{-}L1^+$ lymphocyte was independently associated with good DFS (HR, 0.50; 95% CI, 0.27–0.91, P = .024) (Supplementary Table 8). Patients with high $PD\text{-}L1^+$ lymphocytes had a significantly better 5-year DFS compared with those with low $PD\text{-}L1^+$ lymphocytes (75.7% vs. 48.1%, P < .001) (Supplementary Figure 7).

Discussion

A better understanding of TIME is essential for optimizing the treatment strategy and for designing novel treatment approaches for patients with LARC. Although several studies have evaluated the clinical implication of the TIME of LARCs, they were focused on a limited population of immune cells.

Table 2. Association between the dynamic changes in TIME after preoperative CRT and DFS (n = 101).

	Univariate analysis		Multivariate analysis	
	HR (95% CI)	*P*-value	HR (95% CI)	*P*-value
Age ≥ 65	0.47 (0.17–1.33)	0.15		
Male (vs. Female)	1.51 (0.73–3.13)	0.27		
ypT3–4 (vs. ypT0–2)	1.59 (0.49–5.19)	0.44		
ypN$^+$	3.80 (1.73–8.34)	0.001	3.39 (1.46–7.87)	0.005
Distance of the primary tumor from the anal verge				
> 4 cm	Reference	-		
≤ 4 cm	1.07 (0.54–2.14)	0.85		
Histology				
Well-differentiated	Reference	-		
Others	0.81 (0.29–2.30)	0.70		
Lymphovascular invasion	3.33 (1.63–6.81)	0.001	2.32 (1. 06–5.10)	0.035
Perineural invasion	2.15 (1.09–4.26)	0.028		
Delta parameters* of immune cell subpopulations				
High Δ CD3$^+$ T cell	0.42 (0.21–0.85)	0.016	0.46 (0.22–0.98)	0.043
High Δ CD8$^+$ T cell	0.47 (0.34–0.93)	0.032		
High Δ CD4$^+$ T cell	0.96 (0.50–1.84)	0.90		
High Δ CD4$^+$FoxP3$^+$ regulatory T cell	2.06 (1.04–4.07)	0.037	2.32 (1.09–4.92)	0.028
High Δ CD4$^+$FoxP3$^-$ helper T cell	0.78 (0.40–1.50)	0.45		
High Δ CD20$^+$ B cell	0.38 (0.19–0.78)	0.008	0.54 (0.26–1.13)	0.10
High Δ tumor-associated macrophage	1.02 (0.53–1.96)	0.95		
High Δ M1 macrophage	0.78 (0.40–1.51)	0.46		
High Δ M2 macrophage	1.26 (0.65–2.42)	0.49		
High Δ antigen-presenting cell	1.44 (0.74–2.80)	0.28		
High Δ dendritic cell	0.68 (0.35–1.33)	0.26		
High Δ total lymphocyte (T cell + B cell)	0.54 (0.27–1.06)	0.072		
High Δ PD-L1$^+$ lymphocyte	0.42 (0.21–0.84)	0.014	0.39 (0.17–0.90)	0.027
High Δ PD-L1 $^-$ lymphocyte	0.45 (0.22–0.90)	0.023		
High Δ PD-L1$^+$ tumor cell	1.21 (0.63–2.32)	0.57		

*Delta parameter [Δ] = immune cell subpopulation density after preOP CRT − immune cell subpopulation density at baseline.

Moreover, data on the dynamic changes in the TIME after preoperative CRT in patients with LARC is extremely sparse. This study is, to our knowledge, the most comprehensive analysis of the clinical significance of pretreatment TIME, dynamic changes in the TIME after preoperative CRT, and post-preoperative CRT TIME in patients with LARC.

Recently, immunoscore based on tumor-infiltrating CD3$^+$ and CD8$^+$ T lymphocytes in the pretreatment biopsy samples of LARC patients have been shown to be predictive of the response to neoadjuvant treatment and was significantly associated with survival outcomes.[8] In addition to CD3$^+$ and CD8$^+$ T lymphocytes, a more comprehensive evaluation of various immune cell subpopulations in the TIME was performed in the current study. Furthermore, the evaluation of the clinical significance of immune cell subpopulations was not limited to the tumor compartment but also the stromal compartment. We demonstrated that the immune cells in the tumor compartment were more closely associated with the response to preoperative CRT than the immune cells in the stromal compartment. Higher levels of T-cell subsets (CD3$^+$, CD4$^+$, and CD8$^+$ T cells) and dendritic cells in the tumor compartment were significantly associated with a good response to preoperative CRT. This is in line with previous studies in which tumor-infiltrating lymphocytes including CD3$^+$, CD4$^+$, and CD8$^+$ T cells in the pretreatment biopsy specimens were found to be sensitive predictive markers for response to preoperative CRT.[8,16,17] Regarding CD4$^+$ T cells, we separately evaluated the value of tumor-infiltrating CD4$^+$FoxP3$^-$ helper T cells and CD4$^+$FoxP3$^+$ regulatory T cells. The observation of better response to preoperative CRT in patients with a high density of CD4$^-$FoxP$^-$ helper T cells may be explained by the proposed role of these cells in driving anti-tumor immunity and in supporting anti-tumor CD8$^+$ T cell responses.[18] However, the better response observed in patients with higher levels of CD4$^+$FoxP3$^+$ regulatory T cell is counterintuitive and is contrary to what has been reported for other types of solid tumors.[19,20] Nevertheless, it is important to note that most of the studies that evaluated the prognostic value of tumor-infiltrating CD4$^+$FoxP3$^+$ regulatory T cells in colorectal cancer reported that it is associated with better survival outcomes.[19,21,22] Considering that CD4$^+$ T cells and CD8$^+$ T cells might up-regulate FoxP3$^+$ regulatory T cells, a high density of tumor-infiltrating CD4$^+$FoxP3$^+$ regulatory T cells may reflect a more immune-activated TIME.[23] Indeed, patients with a high density of tumor-infiltrating CD4$^+$FoxP3$^+$ regulatory T cells had higher levels of CD3$^+$ T cells, CD8$^+$ T cells, CD20$^+$ B cells, antigen-presenting cells, and dendritic cells compared with patients with a low density of tumor-infiltrating CD4$^+$FoxP3$^+$ regulatory T cells in the current study. This highlights the importance of a comprehensive assessment of TIME and suggests that the role of specific immune cell populations should be evaluated in conjunction with other immune cell populations.

In addition to the density of immune cells in the TIME, there is growing evidence that the spatial distribution of tumor cells and immune cells is associated with tumor progression and response to treatment.[24,25] A recent study demonstrated that the proximity between CD8$^+$ T cell and tumor cell was associated with better survival outcomes in patients with metastatic colon cancer.[26] In line with this study, our study showed that higher proximity of tumor cells to CD8$^+$ T cells was significantly associated with better response to preoperative

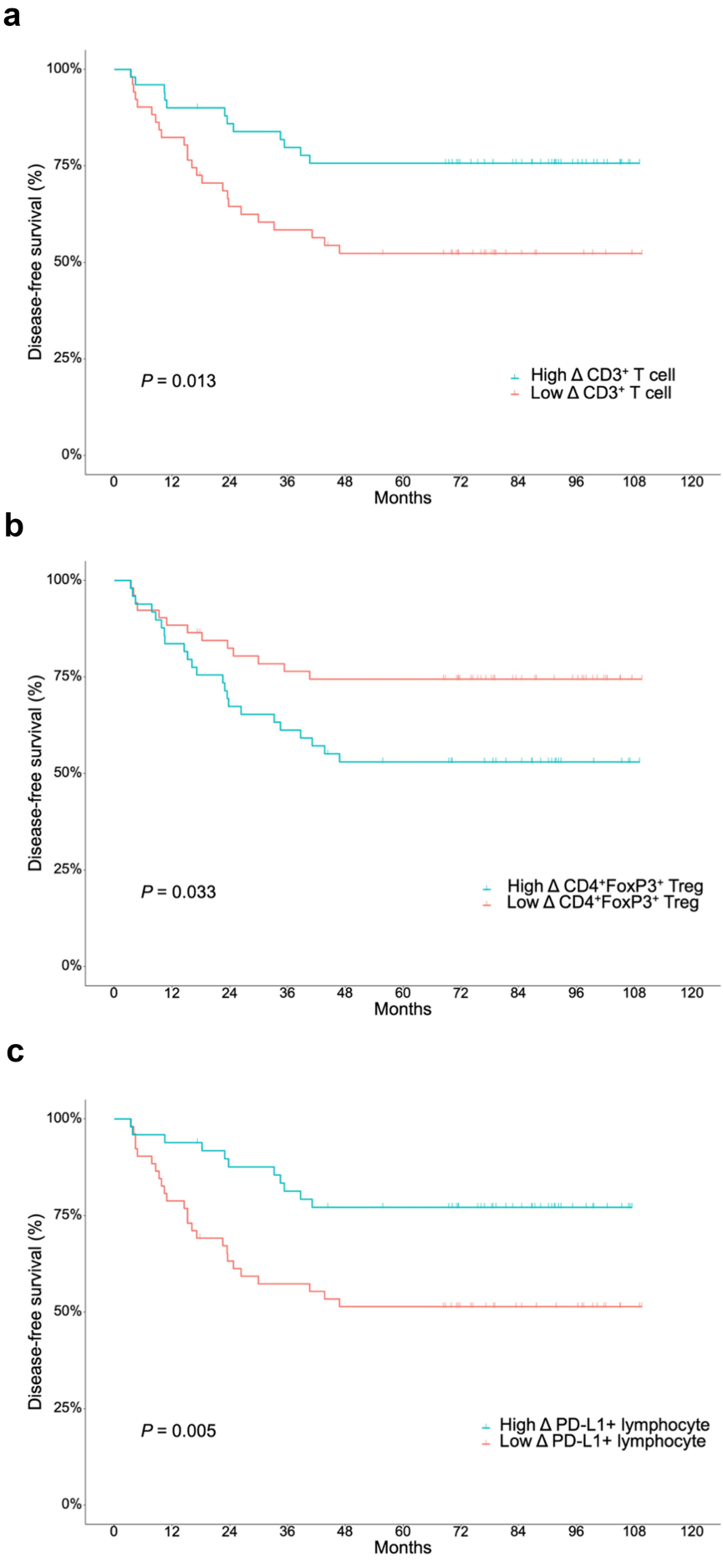

Figure 4. DFS according to dynamic changes in the tumor immune microenvironment after preoperative chemoradiotherapy. a, Δ $CD3^+$ T cells. b, Δ PD-L1 + lymphocytes. c, Δ $CD4^+Fox3^+$ regulatory T cells.

CRT, thereby further supporting the importance of evaluating the spatial distribution of tumor and immune cells in TIME.

Numerous preclinical studies have shown that radiotherapy with or without chemotherapy can induce immunogenic tumor cell death, which is associated with the release of damage-associated molecular patterns, neoantigens, and pro-inflammatory cytokines.[27,28] This leads to the recruitment and activation of dendritic cells as well as the infiltration of T cells into the tumor microenvironment. The present study supports the findings observed in these preclinical studies, as we observed significant increases in the densities of $CD3^+$ T cells, $CD8^+$ T cells, and dendritic cells and a significant decrease in the density of $CD4^+FoxP3^+$ regulatory T cells, indicating that preoperative CRT altered the TIME into a more immune-active status. In addition, a high delta value of $CD3^+$ T cells was associated with good DFS, while a high delta value of $CD4^+FoxP3^+$ regulatory T cells was associated with poor DFS, indicating that the degree of changes in the TIME to an immune-active status by preoperative CRT is correlated with survival outcomes. This significant association between dynamic change in TIME and survival outcome may be because the dynamic changes in the immune cell population may incorporate multiple factors that influence the remodeling of TIME to an anti-tumor immune microenvironment, such as neoantigen load, adequacy of antigen presentation and co-stimulation, and cytokine regulation. Thus, these factors should be evaluated in future studies. In addition, our results may provide evidence to support the combination of CRT and immunotherapy. Indeed, the preliminary report of a recent study showed that CRT followed by immune checkpoint inhibitor prior to surgery was feasible and resulted in a promising pathologic complete remission rate in patients with LARC.[29]

However, there is also evidence from preclinical studies that radiotherapy may induce suppressive immune changes in the TIME, such as the induction of TGFb and IDO1 that leads to an increase in immune-suppressive cells within the TIME such as tumor-associated macrophages.[28] In line with the findings in the preclinical model, we observed that CRT polarized the tumor-associated macrophages from pro-inflammatory M1 macrophages to immune-suppressive M2 macrophages. This suggests that targeting macrophages may result in a synergistic effect with radiotherapy. Indeed, several studies have demonstrated that blocking macrophage recruitment to the TIME or preventing the differentiation of macrophages into an immunosuppressive phenotype resulted in enhanced efficacy of radiotherapy in preclinical models.[28] Another unique finding of the current study is that the density of B cells decreased after preoperative CRT, which may also contribute to the immune-suppressive TIME. Taken together, preoperative CRT changed the TIME into a more immune-active status, but it also had an immune-suppressive aspect.

The clinical significance of PD-L1 expression on lymphocytes has not been well evaluated to date. In the current study, high $PD\text{-}L1^+$ lymphocyte in the pretreatment biopsy sample was significantly associated with good response to preoperative CRT and high delta $PD\text{-}L1^+$ lymphocyte after CRT was associated with good DFS. In addition, high density of $PD\text{-}L1^+$ lymphocytes in surgical specimens after preoperative CRT was also associated with good DFS. The better treatment response and DFS in patients with high $PD\text{-}L1^+$ lymphocytes in the current study suggest that PD-L1 positivity of lymphocytes may have resulted from immune response-induced PD-L1 expression, rather than oncogenic signal-mediated up-regulation of PD-L1, and reflects a more immune-activated TIME.[30,31] Similar findings were observed in a recent study, which demonstrated that PD-L1 expression on immune cells, but not on tumor cells, is a favorable prognostic factor in patients with head and neck cancer.[32] In addition, there was no significant association between $PD\text{-}L1^-$ lymphocytes and response to preoperative CRT or DFS, which further highlights the importance of assessing PD-L1 expression in lymphocytes.

This study has several limitations. Although this study was based on patients who enrolled in the prospective randomized phase II ADORE trial, there may have been a selection bias since this study was a post-hoc analysis on patients treated at a single center, who represent approximately half of the entire ADORE cohort. In addition, according to the study design of the ADORE trial, only patients with ypStage II/III disease after preoperative CRT were included. However, these are the patients who are in most need of TIME assessment as they have a high risk for disease progression that requires optimization of treatment strategies. We also recognize that our pre- and post-treatment sample comparisons may have been influenced by unavoidable sampling bias. Moreover, the underlying mechanism for PD-L1 expression on lymphocytes was not evaluated and needs to be elucidated in future studies. Furthermore, genomic and molecular analyses were not performed. Nevertheless, this study is the first study to comprehensively evaluate the clinical significance of the TIME and the effect of preoperative CRT on the TIME in patients with LARC who were uniformly treated with fluoropyrimidine-based preoperative CRT followed by surgery and adjuvant chemotherapy.

In conclusion, the current study demonstrated that tumor-infiltrating T cells and dendritic cells were associated with the response to preoperative CRT in patients with LARC. Preoperative CRT changed the TIME into a more immune-active status, but it also had an immune-suppressive aspect. The degree of changes in the TIME to immune-active status by preoperative CRT was associated with survival outcomes. A comprehensive assessment of the TIME and the effects of CRT on the TIME in this study provides a framework for future studies incorporating strategies such as immunotherapy to modulate the TIME in patients with LARC.

Acknowledgments

Oxaliplatin, fluorouracil, and leucovorin were kindly provided by SanofiAventis, Korea.

Disclosure statement

The authors declare no potential conflicts of interest.

Funding

This study was funded by Sanofi, Korea. Sanofi did not participate in the conception, conduction or analysis of the trial or the writing of this report.

Data availability statement

The data that support the findings of this study are available from the corresponding author, TWK, upon reasonable request.

References

1. van Gijn W, Marijnen CA, Nagtegaal ID, Kranenbarg EM, Putter H, Wiggers T, Rutten HJ, Påhlman L, Glimelius B, van de Velde CJ, et al. Preoperative radiotherapy combined with total mesorectal excision for resectable rectal cancer: 12-year follow-up of the multicentre, randomised controlled TME trial. Lancet Oncol. 2011;12(6):575–582. doi:10.1016/S1470-2045(11)70097-3
2. Krook JE, Moertel CG, Gunderson LL, Wieand HS, Collins RT, Beart RW, Kubista TP, Poon MA, Meyers WC, Mailliard JA, et al. Effective surgical adjuvant therapy for high-risk rectal carcinoma. N Engl J Med. 1991;324(11):709–715. doi:10.1056/NEJM199103143241101
3. Martling A, Holm T, Rutqvist LE, Johansson H, Moran BJ, Heald RJ, Cedermark B. Impact of a surgical training programme on rectal cancer outcomes in Stockholm. Br J Surg. 2005;92(2):225–229. doi:10.1002/bjs.4834.
4. Kasi A, Abbasi S, Handa S, Al-Rajabi R, Saeed A, Baranda J, Sun W. Total neoadjuvant therapy vs standard therapy in locally advanced rectal cancer: a systematic review and meta-analysis. JAMA Netw Open. 2020;3(12):e2030097. doi:10.1001/jamanetworkopen.2020.30097.
5. Hong YS, Nam BH, Kim KP, Kim JE, Park SJ, Park YS, Park JO, Kim SY, Kim TY, Kim JH, et al. Oxaliplatin, fluorouracil, and leucovorin versus fluorouracil and leucovorin as adjuvant chemotherapy for locally advanced rectal cancer after preoperative chemoradiotherapy (ADORE): an open-label, multicentre, phase 2, randomised controlled trial. Lancet Oncol. 2014;15(11):1245–1253. doi:10.1016/S1470-2045(14)70377-8
6. Hong YS, Kim SY, Lee JS, Nam BH, Kim KP, Kim JE, Park YS, Park JO, Baek JY, Kim TY, et al. Oxaliplatin-based adjuvant chemotherapy for rectal cancer after preoperative chemoradiotherapy (ADORE): long-term results of a randomized controlled trial. J Clin Oncol. 2019;37(33):3111–3123. doi:10.1200/JCO.19.00016
7. Bosset JF, Calais G, Mineur L, Maingon P, Stojanovic-Rundic S, Bensadoun RJ, Bardet E, Beny A, Ollier JC, Bolla M, et al. Fluorouracil-based adjuvant chemotherapy after preoperative chemoradiotherapy in rectal cancer: long-term results of the EORTC 22921 randomised study. Lancet Oncol. 2014;15(2):184–190. doi:10.1016/S1470-2045(13)70599-0
8. El Sissy C, Kirilovsky A, Van den Eynde M, Muşină AM, Anitei MG, Romero A, Marliot F, Junca A, Doyen J, Mlecnik B, et al. A diagnostic biopsy-adapted immunoscore predicts response to neoadjuvant treatment and selects patients with rectal cancer eligible for a watch-and-wait strategy. Clin Cancer Res. 2020;26(19):5198–5207. doi:10.1158/1078-0432.CCR-20-0337
9. Mirjolet C, Charon-Barra C, Ladoire S, Arbez-Gindre F, Bertaut A, Ghiringhelli F, Leroux A, Peiffert D, Borg C, Bosset JF, et al. Tumor lymphocyte immune response to preoperative radiotherapy in locally advanced rectal cancer: the LYMPHOREC study. Oncoimmunology. 2018;7(3):e1396402. doi:10.1080/2162402X.2017.1396402
10. Ogura A, Akiyoshi T, Yamamoto N, Kawachi H, Ishikawa Y, Mori S, Oba K, Nagino M, Fukunaga Y, Ueno M. Pattern of programmed cell death-ligand 1 expression and CD8-positive T-cell infiltration before and after chemoradiotherapy in rectal cancer. Eur J Cancer. 2018;91:11–20. doi:10.1016/j.ejca.2017.12.005
11. Edin S, Kaprio T, Hagström J, Larsson P, Mustonen H, Böckelman C, Strigård K, Gunnarsson U, Haglund C, Palmqvist R. The prognostic importance of CD20$^+$ B lymphocytes in colorectal cancer and the relation to other immune cell subsets. Sci Rep. 2019;9(1):19997. doi:10.1038/s41598-019-56441-8.
12. Yang C, Wei C, Wang S, Shi D, Zhang C, Lin X, Dou R, Xiong B. Elevated CD163$^+$/CD68$^+$ ratio at tumor invasive front is closely associated with aggressive phenotype and poor prognosis in colorectal cancer. Int J Biol Sci. 2019;15(5):984–998. doi:10.7150/ijbs.29836.
13. Ueno H, Ishiguro M, Nakatani E, Ishikawa T, Uetake H, Murotani K, Matsui S, Teramukai S, Sugai T, Ajioka Y, et al. Prognostic value of desmoplastic reaction characterisation in stage II colon cancer: prospective validation in a Phase 3 study (SACURA Trial). Br J Cancer. 2021;124(6):1088–1097. doi:10.1038/s41416-020-01222-8
14. Hendry S, Salgado R, Gevaert T, Russell PA, John T, Thapa B, Christie M, van de Vijver K, Estrada MV, Gonzalez-Ericsson PI, et al. Assessing tumor-infiltrating lymphocytes in solid tumors: a practical review for pathologists and proposal for a standardized method from the International Immunooncology Biomarkers Working Group: part 1: assessing the host immune response, TILs in invasive breast carcinoma and ductal carcinoma in situ, metastatic tumor deposits and areas for further research. Adv Anat Pathol. 2017;24(5):235–251. doi:10.1097/PAP.0000000000000162
15. Dworak O, Keilholz L, Hoffmann A. Pathological features of rectal cancer after preoperative radiochemotherapy. Int J Colorectal Dis. 1997;12(1):19–23. doi:10.1007/s003840050072.
16. Teng F, Meng X, Kong L, Mu D, Zhu H, Liu S, Zhang J, Yu J. Tumor-infiltrating lymphocytes, forkhead box P3, programmed death ligand-1, and cytotoxic T lymphocyte-associated antigen-4 expressions before and after neoadjuvant chemoradiation in rectal cancer. Transl Res. 2015;166(6):721–732. doi:10.1016/j.trsl.2015.06.019.
17. Teng F, Mu D, Meng X, Kong L, Zhu H, Liu S, Zhang J, Yu J. Tumor infiltrating lymphocytes (TILs) before and after neoadjuvant chemoradiotherapy and its clinical utility for rectal cancer. Am J Cancer Res. 2015;5:2064–2074.
18. Tay RE, Richardson EK, Toh HC. Revisiting the role of CD4$^+$ T cells in cancer immunotherapy-new insights into old paradigms. Cancer Gene Ther. 2021;28(1–2):5–17. doi:10.1038/s41417-020-0183-x.
19. Huang Y, Liao H, Zhang Y, Yuan R, Wang F, Gao Y, Wang P, Du Z. Prognostic value of tumor-infiltrating FoxP3$^+$ T cells in gastrointestinal cancers: a meta analysis. PLoS One. 2014;9(5):e94376. doi:10.1371/journal.pone.0094376.
20. Bates GJ, Fox SB, Han C, Leek RD, Garcia JF, Harris AL, Banham AH. Quantification of regulatory T cells enables the identification of high-risk breast cancer patients and those at risk of late relapse. J Clin Oncol. 2006;24(34):5373–5380. doi:10.1200/JCO.2006.05.9584.
21. Kuwahara T, Hazama S, Suzuki N, Yoshida S, Tomochika S, Nakagami Y, Matsui H, Shindo Y, Kanekiyo S, Tokumitsu Y, et al. Intratumoural-infiltrating CD4 + and FOXP3 + T cells as strong positive predictive markers for the prognosis of resectable colorectal cancer. Br J Cancer. 2019;121(8):659–665. doi:10.1038/s41416-019-0559-6
22. Salama P, Phillips M, Grieu F, Morris M, Zeps N, Joseph D, Platell C, Iacopetta B. Tumor-infiltrating FOXP3$^+$ T regulatory cells show strong prognostic significance in colorectal cancer. J Clin Oncol. 2009;27(2):186–192. doi:10.1200/JCO.2008.18.7229.
23. Li C, Jiang P, Wei S, Xu X, Wang J. Regulatory T cells in tumor microenvironment: new mechanisms, potential therapeutic strategies and future prospects. Mol Cancer. 2020;19(1):116. doi:10.1186/s12943-020-01234-1.
24. Fridman WH, Pages F, Sautes-Fridman C, Galon J. The immune contexture in human tumours: impact on clinical outcome. Nat Rev Cancer. 2012;12(4):298–306. doi:10.1038/nrc3245.
25. Gentles AJ, Newman AM, Liu CL, Bratman SV, Feng W, Kim D, Nair VS, Xu Y, Khuong A, Hoang CD, et al. The prognostic landscape of genes and infiltrating immune cells across human cancers. Nat Med. 2015;21(8):938–945. doi:10.1038/nm.3909

26. Lazarus J, Maj T, Smith JJ, Perusina Lanfranca M, Rao A, D'Angelica MI, Delrosario L, Girgis A, Schukow C, Shia J, et al. Spatial and phenotypic immune profiling of metastatic colon cancer. JCI Insight. 2018;3(22). doi:10.1172/jci.insight.121932
27. Corrò C, Dutoit V, Koessler T. Emerging trends for radio-immunotherapy in rectal cancer. Cancers. 2021;13(6):1374. doi:10.3390/cancers13061374.
28. Monjazeb AM, Schalper KA, Villarroel-Espindola F, Nguyen A, Shiao SL, Young K. Effects of radiation on the tumor microenvironment. Semin Radiat Oncol. 2020;30(2):145–157. doi:10.1016/j.semradonc.2019.12.004.
29. Yoshino T, Bando H, Tsukada Y, Inamori K, Yuki S, Komatsu Y, Homma S, Uemura M, Kato T, Kotani D, et al. Voltage: investigator-initiated clinical trial of nivolumab monotherapy and subsequent radical surgery following preoperative chemoradiotherapy in patients with microsatellite stable locally advanced rectal cancer. J Clin Oncol. 2019;37(15 Suppl):3606. doi:10.1200/JCO.2019.37.15_suppl.3606
30. Yi M, Niu M, Xu L, Luo S, Wu K. Regulation of PD-L1 expression in the tumor microenvironment. J Hematol Oncol. 2021;14(1):10. doi:10.1186/s13045-020-01027-5.
31. Chen S, Crabill GA, Pritchard TS, McMiller TL, Wei P, Pardoll DM, Pan F, Topalian SL. Mechanisms regulating PD-L1 expression on tumor and immune cells. J Immunother Cancer. 2019;7(1):305. doi:10.1186/s40425-019-0770-2.
32. Kim HR, Ha SJ, Hong MH, Heo SJ, Koh YW, Choi EC, Kim EK, Pyo KH, Jung I, Seo D, et al. PD-L1 expression on immune cells, but not on tumor cells, is a favorable prognostic factor for head and neck cancer patients. Sci Rep. 2016;6:36956. doi:10.1038/srep36956